

A 120 kHz High-Frequency MOSFET Charging Circuit Using Series Parallel Resonant Converter

Naufal Abdul Aziz Nuawi*, Ermeey Abdul Kadir and Mohammad Nawawi Seroji

Abstract— This paper proposes a new circuit topology of high frequency switching DC-DC Series Parallel Loaded Resonant Converter (SPLRC) at 120 KHz. The circuit is used for a wireless power transmission application that requires a fast-charging operation. The purposed circuit that used a series parallel loaded technique is transformed into a different equivalent circuit for mathematical analysis that efficiently analyses the operation of the circuit in AC and DC modes. For each equivalent circuit, the operation is described and explained. A full detailed circuit calculation using Matlab R2018A is then carried out to determine the purpose converter components' value. Psim software is used to prove the model's validity further. Both computer-based simulations were used to capture the resulting waveform. Initially, the simulation result waveform is captured by using PSIM and then send to Matlab R2018A to plot better. The proposed circuit is fabricated based on the simulation result, and actual experimentation is made. Then a comparison between lab test results and simulations had been made to verify the accuracy of the proposed circuit operation. Furthermore, the targeted 600 W output power can be considered high for a lower voltage input of 24 V, thus, resulting in the resonant tank components value than available in the market. Therefore, the percent error between lab test and simulation is 2.6316% for voltage output. The lower value of output power produces more accurate results rather than the higher value of output power. Most of the components are using low-cost and commercially available in the market. All the finding is explained and discussed from the simulation result, it is confirmed that a high-frequency switching circuit is operated as expected.

Index Terms—DC-DC Converter, SPLRC, MOSFET, Matlab R2018A, Psim, Resonant Converter

This manuscript is submitted on 9th September 202 and accepted on 26th May 2022. This work was funded by Ministry of Higher Education & Research Management Institute (RMI), Universiti Teknologi Mara (UiTM) Fundamental Research Grant Scheme (FRGS) No: 600-IRMI/FRGS 5/3 (045/2019).

N. A. A. Nuawi and M. N. Seroji are with the School of Electrical Engineering, College of Engineering, Universiti Teknologi MARA, 40450, Shah Alam, Selangor. E. A. Kadir is with the School of Electrical Engineering, College of Engineering, Universiti Teknologi MARA, Dungun Campus, 23000, Dungun, Terengganu.

*Corresponding author
Email address: naufalnuawi_95@yahoo.com

1985-5389/© 2021 The Authors. Published by UiTM Press. This is an open access article under the CC BY-NC-ND license (<http://creativecommons.org/licenses/by-nc-nd/4.0/>).

I. INTRODUCTION

NOWADAYS, a high-frequency driver in wireless power transfer, has been widely used, especially since the advent of amplitude-modulated radio in the early 20th century. Nevertheless, due to friction contacts, conventional conductive power interfaces affect the traditional conductive power efficiency of devices and restrict their use or render them unacceptable[1].

An efficient wireless power transfer method would enable advancements in various fields, including embedded computing, mobile computing, sensor networks, and micro robotics[2]. Typically, in wireless power transmission, the signal's frequency must be higher than the standard 50Hz. In an electrical transmission system, it raises series impedance. As a result of the reduced power transfer capabilities, thus, unable to realize the benefits of the transmission system. Most hard switching converters are inefficient, with bulky magnetics resulting in a low switching frequency[3]. It appears that high power losses are caused by high switching techniques[4]. Since hard-switching requires switching on and off with the full load current, it is prone to high switching losses in DC-DC converters.

Nonetheless, switches in soft-switching resonant DC-DC converters turn on and off only when the voltage across or current through them is zero, thereby minimizing or eliminating switching losses[5]. Resonant converters are increasing steadily with a quicker transient response due to the benefits of smaller size and lighter weight[6]. Furthermore, resonant converters are ideal candidates to achieve zero current switchings (ZCS)[7]. Previous researchers proposed a different technique and approach as a solution to the problem. This paper will primarily focus on the development of an advanced power converter for wireless power transfer focusing on switching frequency of 120 kHz and voltage output. The proposed driver comprises a high-frequency DC-AC converter with a design example of a 240 V supply and a 24 V DC input produced by an adapter. In general, the energy dissipation in a power inverter increases as the operating frequency increases[8]. Following that, an AC to DC converter with a switching frequency of 120k Hz and a 19 V output voltage with a power output converter of 600 W will be used as the second stage[9]. This output voltage level is targeted because the output of this project will be used as the source

input for other devices such as laptops with higher output power or power amplifier. As a result, an advanced DC to AC converter topology for the transmitter side and an AC to DC converter topology for the receiver side will be designed.

A switching technique is very important to control the output produced. Some switching methods can produce a desired waveform of the converter, although, it may contain many harmonics which is not good for electronic devices. 3 major methods exist in resonant converters such as series resonant converter, parallel resonant converter, and series parallel resonant converter. Series resonant converter performance is not controllable at light load and zero loads. It is also insensitive to input voltage levels for a fixed output voltage and current. The parallel resonant converter is a load-sensitive resonant current that implies poor part-load efficiency and is also unfit for high output voltages as the off-state voltages of the rectifier exceed voltage output. To solve the limitation from both series and parallel resonant converter, thus, series parallel resonant converter techniques were used since they had more advantages than others such as the filter capacitor ripple current controlled by appropriate choice of the filter inductor, and therefore the circuit is suitable for high output applications. Takes on the characteristics of a parallel-load converter, most importantly that the output voltage may be regulated at a light and no load.

Power MOSFET is used in high switching applications such as switch-mode power supplies (SMPS), brushless DC motor (BLDM) drives solid state relay, automobile applications, etc. [10]. This paper focused on a high-speed switching circuit that used a high capacity gate and a low voltage value MOSFET, both commercially available with goals to develop and design a high-frequency MOSFET driver capable of driving MOSFET, primarily in class E configurations. Class-E switching power amplifiers have fewer components than other power amplifiers, resulting in high reliability[11]. In addition, the proposed high-speed switching circuit will be developed and tested for wireless power transfer applications.

II. DESIGN OF THE CONVERTER

AC analysis or fundamental frequency analysis (FFA) is the most popular, simple, and effective method of analyzing DC-DC resonant converters [4]. In this method, energy transfer from the source to the load is normally assumed to be contributed only by the fundamental component. Furthermore, the harmonics are neglected. Though this method is approximate and inaccurate, it is preferred due to its simplicity, the lesser computation time for solving, and practical ease of implementation. Hence, researchers continue to use this method for analyzing resonant converters [4], [5]. In this paper, coil design is not considered. Essentially, different mutual inductances, M , with a comparable coil structure, can be achieved while conserving the same coupling coefficient, k [12].

The assumption made for the converter:

1. All the diodes and switches are ideal, and switches communicate linearly.

2. The passive components behave linearly.
3. All resonant components and filter capacitors assumed lossless.

The converter used by following the specifications of 240 V supply, 24 V DC input, 120k Hz switching frequency, 500 μ F DC link capacitor, 500 μ F output capacitor, with 1 μ H output inductor and expected output power of 600 W with 19 V voltage output. This paper focused on the switching frequency and the output voltage produced. WPT is used as the proposed application only and not included in this paper. The power switches that are used for the converter are MOSFETs.

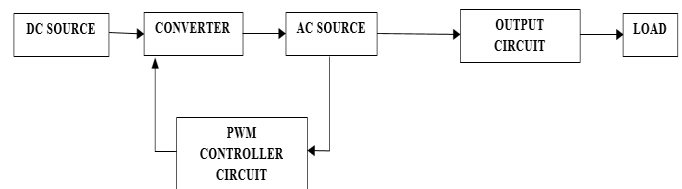


Fig. 1: Block diagram of the proposed converter

Fig. 2 shows the schematic converter of DC-DC SPLRC for wireless power transmission. The design of a resonant converter often starts by designing the resonant network. There are three main parts for the proposed converter which is switching network (square wave generator), resonant tank network, and rectifier network. The resonant network will filter the higher harmonic currents, which helps to produce a sinusoidal current to flow through the resonant network.

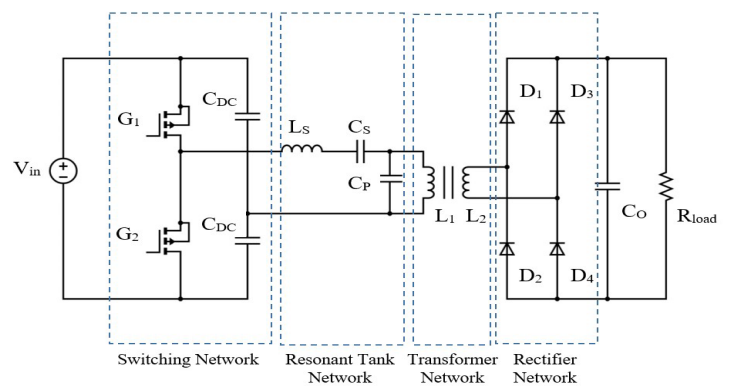


Fig. 2: Simulation for proposed converter using SPLRC.

The fundamental frequency equivalent circuit method as shown in Fig. 3 were used to determine the possible value for the proposed circuit. The sinusoidal input voltage has an amplitude $\frac{2V_{in}}{\pi}$, and the voltage-fed rectifier is substituted with an effective input resistance $R_{eff} = \frac{\pi^2 R}{8}$, which is as same as the parallel resonant converter.

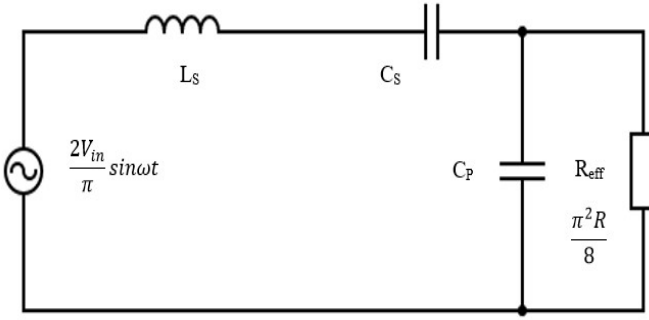


Fig. 3: Fundamental frequency equivalent circuit for the half-bridge of SPLRC.

Resonant frequency, ω_o :

$$\omega_o = \frac{1}{\sqrt{L_s C_s}} = \frac{\omega_s}{\omega_n} \quad (3)$$

- L_s = Inductor series of a resonant tank
- C_s = Capacitor series of a resonant tank
- ω_s = Switching frequency

Where normalized frequency, ω_n :

$$\omega_n = \frac{\omega_s}{\omega_o} \quad (4)$$

The quality factor, Q , of the SPLRC:

$$Q = \frac{\omega_o L_s}{R_l} \quad (5)$$

As component stresses are directly a function of Q , the value of Q should be chosen as low as possible.

$$\left| \frac{V_o}{V_{in}} \right| = \frac{0.5}{\left| \frac{\pi^2}{8} \left[1 + \frac{C_p}{C_s} \left[1 - \omega_n^2 + jQ \left[\omega_n - \frac{1}{\omega_n} \right] \right] \right] \right|} \quad (6)$$

Fig. 4-Fig. 6, gain versus normalized frequency, for SPLRC when the value of $C_p/C_s = 0.5, 1, 2$ which can be used as the quality factor to design the proposed converter. Thus, the proposed design's normalized frequency value, ω_n , from (4) can be obtained from the converter's gain value. The converter value gain obtained is 0.7 by using the 24 V, voltage input and 19 V, voltage output. Since the value of gain for the converter is 0.7, the value for ω_n is 1.6037 for $Q = 0.5$, as shown in Fig. 7. The lower value of Q corresponds to light load condition and higher value for full load condition. The voltage-gain characteristics are important in resonant converter analysis because they help determine the operating region and the values of each resonant feature of the LCC[13].

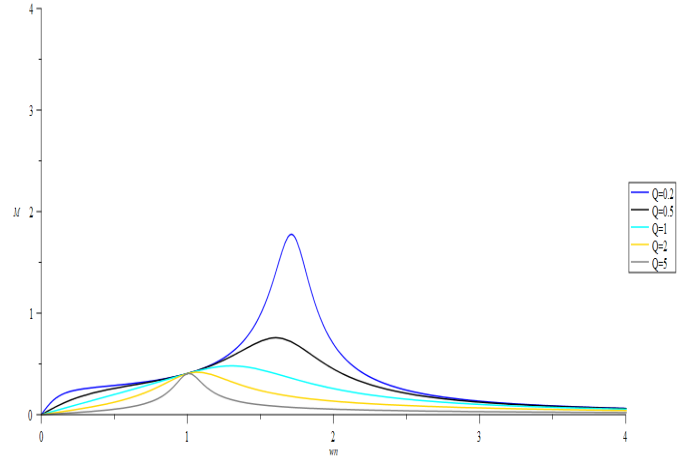


Fig. 4: Gain Curve for SPLRC when $C_p/C_s = 0.5$.

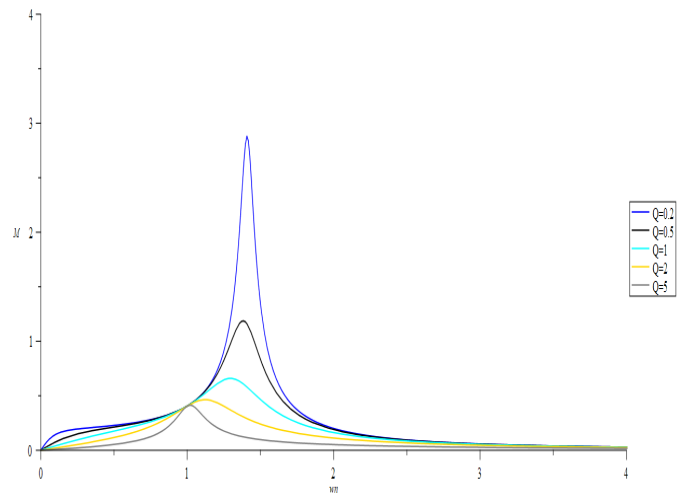


Fig. 5: Gain Curve for SPLRC when $C_p/C_s = 1$.

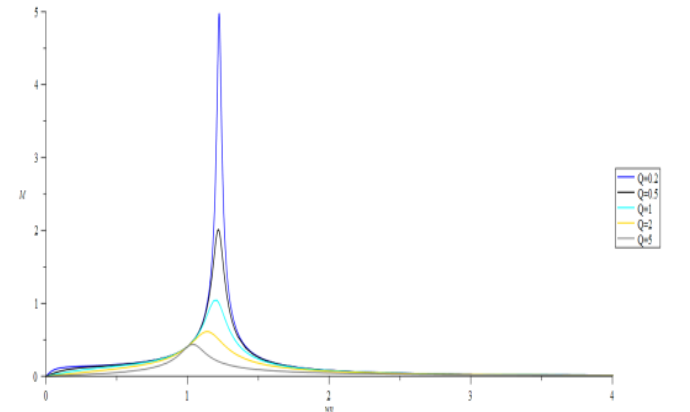


Fig. 6: Gain Curve for SPLRC when $C_p/C_s = 2$.

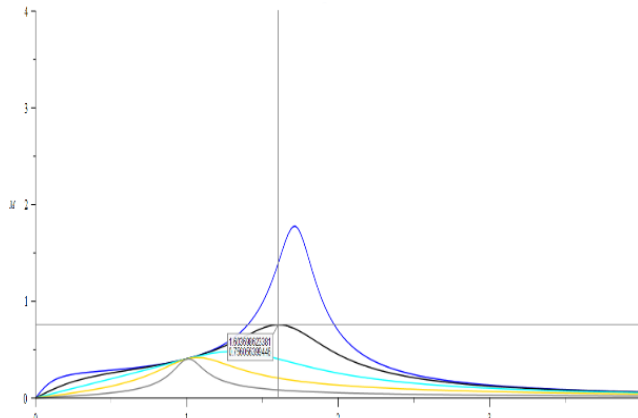


Fig. 7: Gain Curve for SPLRC when $C_p/C_s = 0.5$.

III. RESULTS AND DISCUSSION

This section represents the simulation of the proposed SPLRC. Fig. 9 shows the experimental simulation by using Psim with 24V DC supply at 50 Hz. In this study, a half-bridge of LCC type loaded resonant converter had been implemented. LCC type is shown as Fig. 2 at resonant tank network which one inductor was series to one capacitor and then parallel by one capacitor. The simulation work on suggested SPLRC is performed using 120k Hz of switching frequency, f_s . The value of Q is 0.5 with ω_n of 1.6037, as stated in the previous section. The components value for the design was calculated by using Matlab R2018A as well as experimental components values are listed in Table I. Matlab is used to calculate by using the formula stated in Part II to obtain the actual value for the converter but due to the current market, the components value used for PSIM simulation and experimental at the laboratory is adjusted as stated in Table I. There is two part for components value used in Table I which are calculated for Matlab and simulation values for PSIM and experimental. The comparison of the results is between PSIM simulation and experimental as Table II stated.

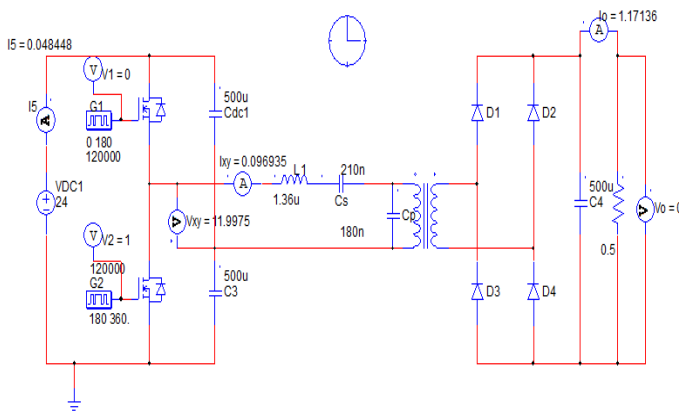


Fig. 8: Simulation circuit of SPLRC by using Psim

Firstly, the driver for the half-bridge rectifier was constructed to meet the required switching frequency of 120 kHz, as shown in Fig. 10. There is 3 part for this driver which

are CD4046, HEF4049BP, and IR2110. The signal illustrated for the two MOSFETs used was proved by the signal shown in Fig. 11.

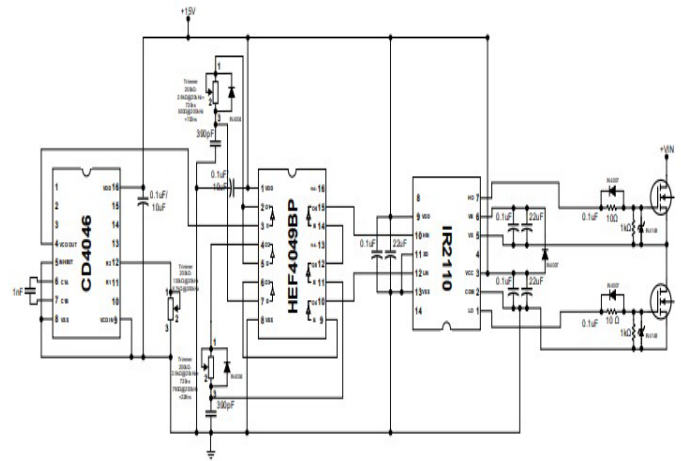
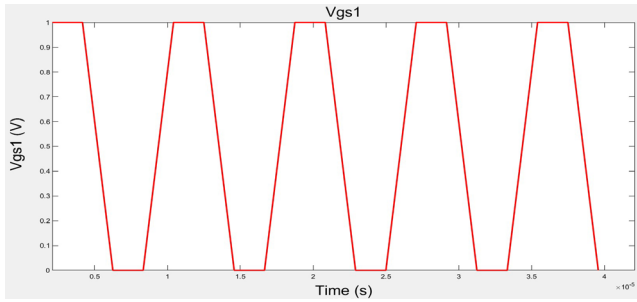


Fig. 9: Circuit Driver for Half-Bridge Rectifier

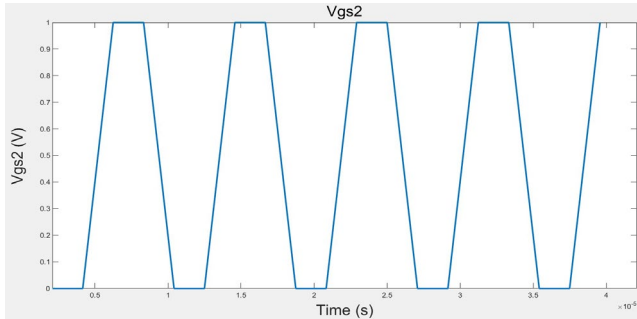
TABLE I
COMPONENTS VALUE OF THE CONVERTER FROM CALCULATION AND SIMULATION

Parameter	CALCULATED	Simulation
Supply Voltage, V_s	240 V	240V
Voltage Input, V_m	24 V	24V
Voltage Output, V_o	19 V	19V
Power Output, P_o	600 W	600W
Quality Factor, Q	0.5	0.5
Switching Frequency, f_s	120000 Hz	120000 Hz
Switching Frequency, Ω_s	753.982 k rad/sec	753.982 k rad/sec
Gain, M	0.79167	0.79167
Normalized Frequency, Ω_n	1.6037 rad/sec	1.6037 rad/sec
Load Resistor, R	0.60167 Ω	0.5 Ω
Effective Input Resistance, R_e	0.74228 Ω	-
Resonant Frequency, Ω_o	470.152 k rad/sec	-
Capacitor Series, C_s	0.1452 μF	210nF
Capacitor Parallel, C_p	0.7258 μF	180nF
Inductor Series, L_s	0.7894 μH	1.36 μH
Capacitor Output, C_o	500 μF	500 μF
DC-Link Capacitor, C_{DC}	500 μF	500 μF

A straightforward technique to understand resonant topologies' characteristics is by looking at their gain curve plot, as discussed in part II. The curves show that the controller will not regulate the output voltage if the resonant converter operates above the resonant frequency (the right side of the gain curve). The curves also imply that Q decreases as the load increases. The gain curve becomes flat, and, hence, major frequency modifications are expected to ensure the desired output voltage. Therefore, open circuit control is unlikely even if there is no resonant peak or selectivity. The high Q value is desirable to achieve better control in the series resonant converter. The trade-off, however, is that if Q is too high, then the output control mechanism becomes non-linear. The minor shift in the switching frequency will produce a significant change in the output voltage, and the operating frequency also could be shifted quite near to the resonant peak by the circuit. The condition destabilizes the power supply in turn.



a) High side input for MOSFET 1



b) Low side input for MOSFET 2

Fig. 10: Simulation for switching frequency of two MOSFETs

As shown in Fig. 10, the simulation waveform was obtained for two MOSFETs of the high side and low side by using a 120 kHz switching frequency. The simulation can be proven successfully as the experimental result shows that the same waveform for switching frequency as shown in Fig. 11 with a dead time of 80 ns. Ideally, the dead time for switching frequency is 50 ns but depends on the switching frequency used.



Fig. 11: Signal for high side input (H_{in}) and low side input (L_{in}) from MOSFET Driver

Fig. 11 depicts the conditioned ON and OFF signal between the two MOSFETs as shown in Fig. 9 and compared

to the simulation results as shown in Fig. 10. When G1, for high side MOSFET, is On, G2, for low side MOSFET, will be in an OFF state. Thus the resonant current I_{xy} , naturally falls to zero and the component D1 may be switched off whilst the anti-parallel D1 diode is conducting due to the resonant current I_{xy} , being negative and G2 is yet to be turned on. The turn-off loss is zero and there are no abrupt voltage and current changes. This is known as Zero-Current-Switching (ZCS). However, the transistor turn-on is similar to in conventional square wave converter. The transistor's turn-off condition is similar to the conventional square wave converter as the loss exists during turn-off in switching devices.

In Fig. 13, the square wave will be injected into the resonant network labeled as V_{xy} . Based on Fig. 12, the voltage and current overlap thus hard switching occurs when the transistor is on and off state. Since the resonance factor occurred, the square wave was automatically converted into the sinusoidal waveform when entering the resonant network. Then, the primary current that flows through the resonant tank will also be in sinusoidal type. After the resonant tank, the current will be rectified to get DC output.

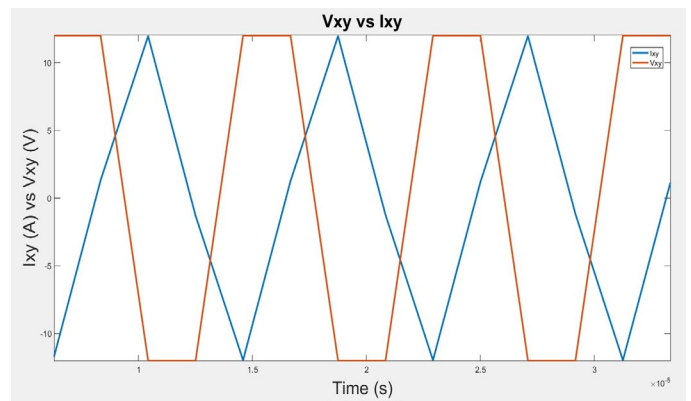


Fig. 12: Resonant tank voltage, V_{xy} , and current, I_{xy} .

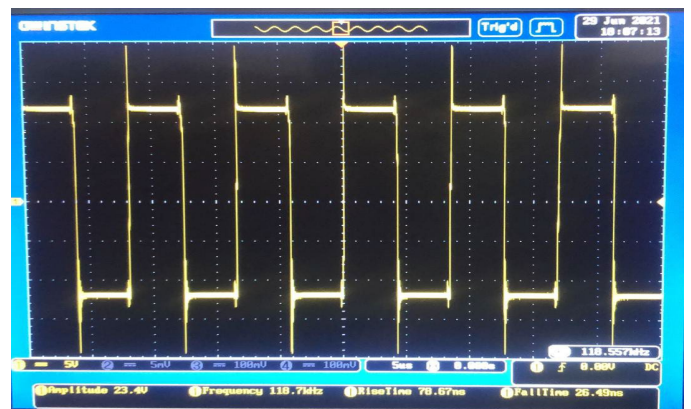


Fig. 13: Experimental result for resonant tank voltage, V_{xy} , signal.

The converter will work with a very low Q to avoid the non-linear gain curve characteristics, so the curve should be

flat at almost any frequency, as reported in Fig. 14. Even more observation of Fig. 14 poses the issue of regulating the output voltage. Thus, the proposed design solves the problem of controlling the output when the voltage stays the same at either frequency. A parallel capacitor is placed after a series of inductors and capacitors at a resonant tank. To control the output voltage, the filter capacitor ripples current is governed by the appropriate choice of the filter inductor. Therefore the circuit is suitable for low output applications, as shown in Fig. 15. It takes on a parallel-load converter's characteristics, most notably that the output voltage may be regulated at the light and no load. In the case of the two switches or MOSFET operating above the resonant frequency, F_o , the resonant tank, now acts as inductive impedance resulting in the resonant current, I_{xy} lags the resonant voltage, V_{xy} , as illustrated in Fig. 12.

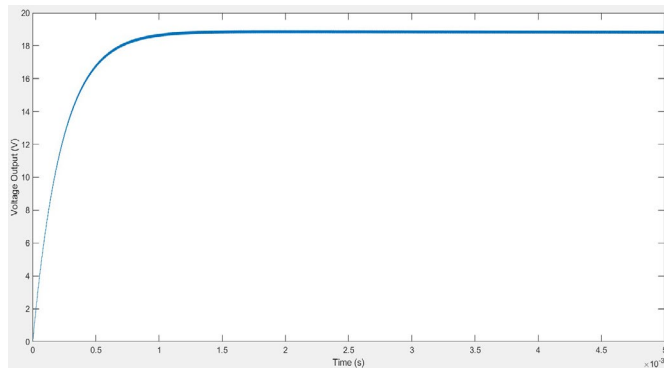


Fig. 14: Output Voltage

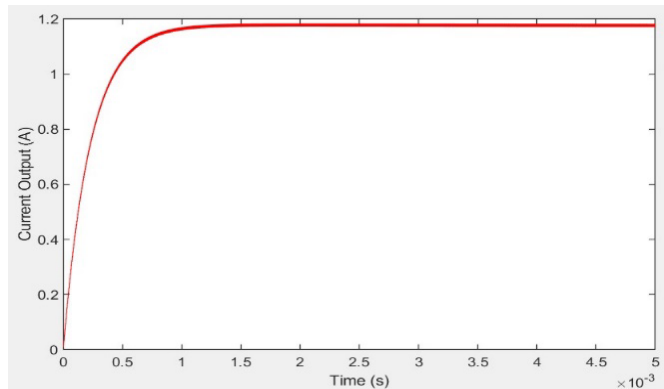


Fig. 15: Output Current

In this paper, the research focused on the switching frequency and the output voltage. The results of simulation of SPLRC using simulation and experimentally shown as Table II for voltage output and current output. The percent error between simulation and experimental voltage output is 2.6316% since the value used between simulations and experimental is different. Previous researchers stated that when the total transmission power to the main and auxiliary batteries was 1100 W, the greatest percentage errors in transmission power and resonant circuit loss were 7.2% and 0.8%, respectively, in Primary-side Coupled Mode[14]. As detailed in the table, the current output shows the wide gap between simulation and experimental. The actual output of the current is 31.579 A by using the ohms law equation. Since the

value for the components was adjusted, the current produced by the proposed converter is 1.1736 A (simulation) and 0.037 A (experimental) as shown in Table II. Current output cannot be identified properly due to the lack of equipment at the laboratory. Future work may be done appropriately by using a current probe to improve the result on the current output.

TABLE II
RESULTS OF THE SIMULATION AND EXPERIMENTAL

Parameter	SIMULATION	Experimental
Voltage output, V_o	19V	18.5V
Current output, I_o	1.1736A	0.037A

IV. CONCLUSION

Each constituent of a half-bridge series-parallel loaded resonant converter was collected and examined. The simulation and experiment outcomes were similar, according to the findings based on switching frequency and voltage output. The output voltage deviates by 0.5% lower than the expected result of 19 V. As a result of the findings, it is possible to conclude that this study effectively designed and produced a half-bridge series-parallel loaded resonant converter according to the proposed objectives. Further work is required to compare the theoretical and simulation results with practical results to confirm the circuit operation and analysis while developing more into WPT to produced better output results. Other possible research work will be studied including the alternative circuit configurations such as full-bridge switching configuration rather than the half-bridge, the closed-loop control, and the efficient method for reducing the output ripple while taking the preminent potential output for current as well as LLC type of resonant network.

V. ACKNOWLEDGMENT

The Financial support from the Ministry of Higher Education & Research Management Institute (RMI), Universiti Teknologi Mara (UiTM) Fundamental Research Grant Scheme (FRGS) No: 600-IRMI/FRGS 5/3 (045/2019), is gratefully acknowledged for implementation of this project.

VI. REFERENCES

- [1] G. Pavlov, I. Vinnichenko, M. Pokrovskiy, and N. Tarabanov, "Electromagnetic Processes in Serial-To-Parallel Resonant Converter for Contactless Charging of Electric Vehicle Battery," *2019 IEEE 39th Int. Conf. Electron. Nanotechnology, ELNANO 2019 - Proc.*, pp. 668–673, 2019, doi: 10.1109/ELNANO.2019.8783649.
- [2] D. D. Stancil and S. C. Goldstein, "Magnetic Resonant Coupling As a Potential Means for Wireless Power Transfer to Multiple Small Receivers," *Ieee Trans. Power Electron.*, vol. 24, no. 7, pp. 1819–1825, 2009, doi: 10.1109/TPEL.2009.2017195.
- [3] D. Patii, A. K. Rathore, D. Srinivasan, and S. K. Panda, "High-frequency soft-switching LCC resonant current-fed DC/DC converter with high voltage gain for DC microgrid application," *IECON Proc. (Industrial Electron. Conf.)*, pp. 4293–4299, 2014, doi: 10.1109/IECON.2014.7049148.
- [4] M. A. Ghalib and Y. S. Abdalla, "Design and Implementation of a Pure Sine Wave Single Phase Inverter for Photovoltaic Applications," *Int. Conf. Informatics, Electron. Vis.*, pp. 1–8, 2013,

doi: 10.1109/ICIEV.2012.6317332.

- [5] M. Khalil-Abaker, J. Shi, and A. Kalam, "Design of a 100W bi-directional LCC series-parallel resonant DC-DC converter," *2016 Australas. Univ. Power Eng. Conf.*, pp. 1–5, 2016, doi: 10.1109/aupec.2016.7749334.
- [6] V. Sivachidambaranathan, "High Frequency Isolated Series Parallel Resonant Converter," vol. 8, no. July, pp. 1–6, 2015, doi: 10.17485/ijst/2015/v8i.
- [7] X. Tan, S. Member, X. Ruan, and S. Member, "Optimal Design of DCM LCC Resonant Converter With Inductive Filter Based on Mode Boundary Map," vol. 30, no. 8, pp. 4144–4155, 2015.
- [8] C. Jiang, K. T. Chau, C. Liu, and C. H. T. Lee, "An overview of resonant circuits for wireless power transfer," *Energies*, vol. 10, no. 7, pp. 1–20, 2017, doi: 10.3390/en10070894.
- [9] Y. H. Huang, T. J. Liang, and W. J. Wu, "Analysis and implementation of half-bridge resonant capacitance LLC converter," *Proc. IEEE Int. Conf. Ind. Technol.*, vol. 2016-May, pp. 1302–1307, 2016, doi: 10.1109/ICIT.2016.7474943.
- [10] M. A. G. H. Prof. S.K.Patil, Prof. T.T.Waghmare, Mr.V.P.Mohale, "High Frequency driver circuit for MOSFET full bridge Resonant Converter," pp. 56–59.
- [11] W. Chen, R. A. Chinga, S. Yoshida, J. Lin, C. Chen, and W. Lo, "A 25.6 W 13.56 MHz wireless power transfer system with a 94% efficiency GaN Class-E power amplifier," *IEEE MTT-S Int. Microw. Symp. Dig.*, pp. 25–27, 2012, doi: 10.1109/MWSYM.2012.6258349.
- [12] X. Liu and S. Y. R. Hui, "Equivalent circuit modeling of a multilayer planar winding array structure for use in a universal contactless battery charging platform," *IEEE Trans. Power Electron.*, vol. 22, no. 1, pp. 21–29, 2007, doi: 10.1109/TPEL.2006.886655.
- [13] M. A. Halim, M. N. Hidayat, and M. N. Seroji, "Implementation and analysis of a half-bridge series-parallel LLC loaded resonant DC-DC converter for low power applications," *Proc. Int. Conf. Power Electron. Drive Syst.*, pp. 634–638, 2013, doi: 10.1109/PEDS.2013.6527096.
- [14] D. S. Nugroho, R. Ota, and N. Hoshi, "A Novel Multi-port Bi-directional Inductive Power Transfer System with Simultaneous Main and Auxiliary Battery Charging Capability," *2019 IEEE 4th Int. Futur. Energy Electron. Conf. IFEEC 2019*, 2019, doi: 10.1109/IFEEC47410.2019.9014930.



Mohammad Nawawi S. completed his joint Master's degree program in Power Electronics and Drives at The University of Birmingham and The University of Nottingham in 2003 and was awarded the doctoral degree in Electrical, Electronics & Computer Engineering in 2008 by The University of Birmingham. He is currently an Associate Professor at the Faculty of Electrical Engineering (FKE), UiTM. His research interests include high frequency power electronic converters, soft-switched resonant converter, high power factor converter, wireless power transfer and micro-energy system.



Naufal Abdul Aziz N. was born in Dungun, Terengganu in 1995. He received his Diploma in Electrical Engineering (Power) in 2015 and B.Eng. (Power) in 2018 from Universiti Teknologi MARA. He is currently a graduate research assistant at Universiti Teknologi MARA. His interests include power electronics and data processing with application to wireless

power transfer. He is also a graduate member of the Board of Engineers Malaysia (BEM).



Ermee Abdul K. is a Doctoral degree holder from the school of Electrical and Computer engineering at The University of Auckland (2016). His researches are in electronics, communication engineering, renewable energy, and energy harvesting systems. The system's application on a low power energy harvesting system has been tackled recently. He is affiliated with IEEE

as a student member. In IET and other scientific publications, he has served as an invited reviewer.